Ocean Engineering Vol 38, 2011, pp. 341-359

Practical aspects of frequency-domain identification of dynamic models of marine structures from hydrodynamic data

Tristan Perez [a,c,*], Thor I. Fossen [b,c]

[a] School of Engineering—Mechanical and Mechatronics, The University of Newcastle, Callaghan, NSW 2308, Australia
[b] Department of Engineering Cybernetics, Norwegian University of Science and Technology (NTNU), NO-7491 Trondheim, Norway
[c] Centre for Ships and Ocean Structures (CeSOS), Norwegian University of Science and Technology (NTNU), NO-7491 Trondheim, Norway

A B S T R A C T

The motion response of marine structures in waves can be studied using finite-dimensional linear-time-invariant approximating models. These models, obtained using system identification with data computed by hydrodynamic codes, find application in offshore training simulators, hardware-in-the-loop simulators for positioning control testing, and also in initial designs of wave-energy conversion devices. Different proposals have appeared in the literature to address the identification problem in both time and frequency domains, and recent work has highlighted the superiority of the frequency-domain methods. This paper summarises practical frequency-domain estimation algorithms that use constraints on model structure and parameters to refine the search of approximating parametric models. Practical issues associated with the identification are discussed, including the influence of radiation model accuracy in force-to-motion models, which are usually the ultimate modelling objective. The illustration examples in the paper are obtained using a freely available MATLAB toolbox developed by the authors, which implements the estimation algorithms described.

Keywords:
System identification
Fluid-memory models
Radiation-force models
Time-domain seakeeping models

1. Introduction

Linear models for the description of motion of marine structures are the basis of training simulators for offshore operations and hardware-in-the-loop testing simulators for positioning control of offshore vessels and oil rigs. These models are also used for initial design and prediction of power capture of wave-energy converters. Once a linear model is obtained, non-linear terms capturing viscous effects can be added to improve the quality of the model.

One approach used to develop linear time-domain models of marine structures consist of using potential theory to compute frequency-dependent coefficients and frequency responses (non-parametric models), and then use these data to either implement the Cummins equation or to apply system identification to obtain a parametric model that approximates the Cummins equation. The latter leads to state-space representations that have advantages in terms of analysis of dynamic behaviour and simulation speed, which can improve up to two orders of magnitude depending on the number of degrees of freedom considered (Taghipour et al., 2008). A great deal of work has been reported in the literature proposing the use of different identification methods to obtain approximating models—see, for example, Jefferys et al. (1984), Jefferys and Goheen (1992), Yu and Falnes (1995, 1998), Holappa and Falzarano (1999), Hjulstad et al. (2004), Kristansen and Egeland (2003), Kristiansen et al. (2005), Jordan and Beltran-Aguedo (2004), McCabe et al. (2005), and Sutulo and Guedes-Soares (2005). Not all of the proposed methods lead to approximating models that satisfy the physical properties associated with the hydrodynamic phenomena involved. This motivated the work of Perez and Fossen (2008b), in which appropriate constraints on the model structure derived from the radiation potential properties were used to expand the work of McCabe et al. (2005). The use of constraints in the identification process refines the search for models and improves the quality of the approximations. This work was then extended in Perez and Fossen (2008a) to the case where the infinite-frequency added mass coefficients are not available—this is the case of most commercial strip-theory codes.

In this paper, we summarise the estimation algorithms developed in Perez and Fossen (2008a, 2008b). We then discuss practical aspects of the identification; and in particular, the influence of radiation model accuracy on the force-to-motion models. The illustration examples in the paper are obtained using the MSS-FDI toolbox, which is a free toolbox for identification of radiation forces of marine structures available at www.marinecontrol.org.

2. A linear model based on the Cummins equation

The linearised equation of motion of marine structure can be formulated as

$$\mathbf{M}\ddot{\boldsymbol{\xi}} = \boldsymbol{\tau}. \tag{1}$$

The matrix $\mathbf{M}$ is the rigid-body generalised mass. The generalised-displacement vector $\boldsymbol{\xi} \triangleq [x,y,z,\phi,\theta,\psi]^T$ gives the position (x-surge, y-sway, and z-heave) of the body-fixed frame with respect to an equilibrium frame and the orientation in terms of Euler angles (ϕ-roll, θ-pitch, and ψ-yaw). The generalised force vector and $\boldsymbol{\tau} \triangleq [X,Y,Z,K,M,N]^T$ give the respective forces and moments in the six degrees of freedom. This force vector can be separated into three components:

$$\boldsymbol{\tau} = \boldsymbol{\tau}_{rad} + \boldsymbol{\tau}_{res} + \boldsymbol{\tau}_{exc}, \tag{2}$$

where the first component corresponds to the radiation forces arising from the change in momentum of the fluid due to the motion of the structure, the second are restoring forces due to gravity and buoyancy, and the third component represents the pressure forces due to the incoming waves, which accounts for Froude–Krylov (pressure forces due to the undisturbed wave field) and diffraction forces (arising from the modification of wave field due to the presence of the structure).

Cummins (1962) studied the radiation hydrodynamic problem in an ideal fluid in the time-domain. For zero-forward speed case, the linear pressure-induced radiation forces can be expressed as

$$\boldsymbol{\tau}_{rad} = -\mathbf{A}_\infty \ddot{\boldsymbol{\xi}} - \int_0^t \mathbf{K}(t-t')\dot{\boldsymbol{\xi}}(t')\,dt'. \tag{3}$$

The first term in (3) represents pressure forces due to the accelerations of the structure. The parameter $\mathbf{A}_\infty$ is a constant positive-definite matrix, in which the entries are the *added mass* coefficients. The second term represents fluid-memory effects that capture the energy transfer from the motion of the structure into the fluid in terms of radiated waves on the free surface. The convolution term is known as a *fluid-memory model*. The kernel of the convolution term, $\mathbf{K}(t)$, is the matrix of *retardation* or *memory functions* (impulse responses).

By combining terms and adding the linearised restoring forces $\boldsymbol{\tau}_{res} = -\mathbf{G}\boldsymbol{\xi}$, the *Cummins Equation* (Cummins, 1962) is obtained:

$$(\mathbf{M}+\mathbf{A}_\infty)\ddot{\boldsymbol{\xi}} + \int_0^t \mathbf{K}(t-t')\dot{\boldsymbol{\xi}}(t')\,dt' + \mathbf{G}\boldsymbol{\xi} = \boldsymbol{\tau}_{exc}, \tag{4}$$

Eq. (4) describes the motion of the structure for any wave excitation $\boldsymbol{\tau}_{exc}(t)$ provided the linearity assumption is satisfied; and it forms the basis of more complex models, which can be obtained by adding non-linear terms to represent different physical effects such as viscous damping and non-linear restoring terms due to mooring lines.

When the radiation forces (3) are considered in the frequency domain, they can be expressed as follows (Newman, 1977; Faltinsen, 1990):

$$\boldsymbol{\tau}_{rad}(j\omega) = \omega^2\mathbf{A}(\omega)\boldsymbol{\xi}(j\omega) - j\omega\mathbf{B}(\omega)\boldsymbol{\xi}(j\omega). \tag{5}$$

The parameters $\mathbf{A}(\omega)$ and $\mathbf{B}(\omega)$ are the frequency-dependent added mass and potential damping, respectively. This representation leads to the following frequency-domain relationship between the excitation forces and the displacements:

$$[-\omega^2[\mathbf{M}+\mathbf{A}(\omega)] + j\omega\mathbf{B}(\omega) + \mathbf{G}]\boldsymbol{\xi}(j\omega) = \boldsymbol{\tau}_{exc}(j\omega). \tag{6}$$

Ogilvie (1964) showed the relation between the parameters of the time-domain model (4) and the frequency-domain model (6) using the Fourier transform of (4):

$$\mathbf{A}(\omega) = \mathbf{A}_\infty - \frac{1}{\omega}\int_0^\infty \mathbf{K}(t)\sin(\omega t)\,dt, \tag{7}$$

$$\mathbf{B}(\omega) = \int_0^\infty \mathbf{K}(t)\cos(\omega t)\,dt. \tag{8}$$

From expression (7) and the application of the Riemann–Lebesgue lemma, it follows that $\mathbf{A}_\infty = \lim_{\omega\to\infty}\mathbf{A}(\omega)$, and hence $\mathbf{A}_\infty$ is called infinite-frequency added mass.

It also follows from the Fourier transform that the time- and frequency-domain representations of the retardation functions are

$$\mathbf{K}(t) = \frac{2}{\pi}\int_0^\infty \mathbf{B}(\omega)\cos(\omega t)\,d\omega, \tag{9}$$

and

$$\mathbf{K}(j\omega) = \int_0^\infty \mathbf{K}(t)e^{-j\omega t}\,d\omega = \mathbf{B}(\omega) + j\omega[\mathbf{A}(\omega) - \mathbf{A}_\infty]. \tag{10}$$

Expressions (9) and (10) are key to generate the data used in the identification problems that seek parametric approximations to the fluid-memory terms.

Hydrodynamic codes based on potential theory, are nowadays readily to compute $\mathbf{B}(\omega)$ and $\mathbf{A}(\omega)$ for a finite set of frequencies of interest—see, for example, Beck and Reed (2001) for an overview of the characteristics of these codes. Commercially available hydrodynamic codes based on 3D potential theory often solve the boundary-value problem associated with infinite-frequency that gives $\mathbf{A}_\infty$. For slender vessels, codes based on strip theory (2D) can be used. Slenderness results in the velocity field being nearly constant along the longitudinal direction, and this characteristic allows reducing the 3D problem to a 2D problem (Newman, 1977). The 2D hydrodynamic problem associated with each section or strip of the hull can be solved, for example, using conformal mapping or panel methods. For an example of a commonly used strip-theory formulation, see Salvesen et al. (1970).

3. Parametric approximations

A direct approach to use non-parametric models to implement simulation models consists of a direct implementation of (4) in discrete time. This approach can be time consuming in simulations and may require significant amounts of computer memory as demonstrated in Taghipour et al. (2008). In addition, the non-parametric models can result difficult to work with for the analysis of stability of the equations of motion. One way to overcome these difficulties consists of approximating the fluid-memory models by a linear-time-invariant parametric model in state-space form:

$$\boldsymbol{\mu} = \int_0^t \mathbf{K}(t-t')\dot{\boldsymbol{\xi}}(t')\,dt' \approx \begin{array}{l} \dot{\mathbf{x}} = \hat{\mathbf{A}}\mathbf{x} + \hat{\mathbf{B}}\dot{\boldsymbol{\xi}}, \\ \hat{\boldsymbol{\mu}} = \hat{\mathbf{C}}\mathbf{x}, \end{array} \tag{11}$$

where the number of components of the state vector $\mathbf{x}$ corresponds to the order of the approximating system and the matrices $\hat{\mathbf{A}}$, $\hat{\mathbf{B}}$, and $\hat{\mathbf{C}}$ are constants.

From a simulation point of view, the advantage of the state-space model lies in the Markovian property of the model, namely, at any time instant, the values of the state $\mathbf{x}$ summarise all the past information of the system. Hence, it is only necessary to store the state vector of the model. Taghipour et al. (2008), considered as an example a time-domain model corresponding to the vertical motion of a container ship (four convolutions—coupled in heave–pitch), and obtained increases in simulation speed of 40 times when using state-space models with respect to models using the convolution integral. Similarly, Taghipour et al. (2007), showed an increase in simulation speeds of 80 times for a flexible structure. The gain in simulation speed becomes more significant as the complexity of the model increases.

The approximating state-space model (11) can be obtained using system identification. This procedure is not new for the problems considered in this paper, and there has been a significant amount of literature dedicated to this problem during the last 20 years. The reason for this is that the identification problem can be posed either in the time or in the frequency domain depending on whether (9) or (10) are used to generate the data for identification. The recent work of Perez and Fossen (2008b) highlights the

superiority of the frequency-domain methods in terms of accuracy and ease of implementation of the estimation algorithms. In this mentioned work, constraints on the model structure derived from the radiation potential properties are used to expand the work of McCabe et al. (2005) and also to simplify the estimation algorithm by reducing it to sequence of linear least-square optimisation problems. The frequency-domain identification seeks rational transfer function approximations:

$$\hat{K}_{ik}(s) = \frac{P_{ik}(s)}{Q_{ik}(s)} = \frac{p_r s^r + p_{r-1}s^{r-1} + \cdots + p_0}{s^n + q_{n-1}s^{n-1} + \cdots + q_0}. \tag{12}$$

By restricting s to take only imaginary values, $s = j\omega$, we obtain the frequency response of the model. The coefficients of (12) are determined such that this frequency response approximates the one given by (10). Once the coefficients of the transfer functions are obtained, a state-space realisation can be obtained using any of the standard canonical forms—see, for example, Kailath (1980).

4. Constraints on parametric approximations

An important aspect of any identification problem is the amount of *a priori* information available about the dynamic system under study and how this information is used in the identification method to set constraints on the model structure and parameters. Table 1 shows on the left-hand side column five properties of the fluid memory models. These properties were derived by Perez and Fossen (2008b) using hydrodynamic properties of the radiation potential. The right-hand side column of Table 1 summarises implications the properties have on the parametric model approximations (12).

The low-frequency asymptotic value (property 1 in Table 1), establishes that the transfer functions $\hat{K}_{ik}(s)$ in (12) have a zero at $s=0$. This can be used to set the constraint $b_0=0$ in (12):

$$\hat{K}_{ik}(s) = \frac{P_{ik}(s)}{Q_{ik}(s)} = \frac{p_r s^r + p_{r-1}s^{r-1} + \cdots + p_1 s}{s^n + q_{n-1}s^{n-1} + \cdots + q_0}. \tag{13}$$

The high-frequency asymptotic value (property 2 in Table 1) establishes that the transfer function models are strictly proper, that is $\deg(Q_{ik}) > \deg(P_{ik})$ since this result in the denominator growing faster than the numerator as the frequency increases, and hence, the frequency response tends asymptotically to zero. The initial-time value (property 3 in Table 1), however, imposes a further constrain on the relative degree. This property establishes that the relative degree of $\hat{K}_{ik}(s)$ is exactly 1. Indeed, for the entries $K_{ik}(j\omega)$ that are not uniformly zero due to symmetry of the hull, the initial-value theorem of the Laplace transform establishes that

$$\begin{aligned}\lim_{t\to 0^+} \hat{K}_{ik}(t) &= \frac{2}{\pi}\int_0^\infty B_{ik}(\omega)\, d\omega \neq 0,\\ &= \lim_{s\to\infty} s\hat{K}_{ik}(s) = \lim_{s\to\infty} s\frac{P_{ik}(s)}{Q_{ik}(s)} = \frac{s^{r+1}p_r}{s^n}.\end{aligned} \tag{14}$$

This will hold if $n=r+1$. Hence, the relative degree of the approximations must be 1, that is $\deg(Q_{ik})-\deg(P_{ik})=1$. The final-time value (property 4 in Table 1) establishes that the impulse response tends to zero as time goes to infinity. This is a necessary and sufficient condition of bounded-input bounded-output stability of the models. With regards to the property 5 in Table 1, the negative feedback interconnection of passive systems is passive; and thus, stable under observability conditions (Khalil, 2000)—further details about passivity of fluid-memory models of marine structures are given, for example, in Damaren (2000). Fig. 1 shows a block diagram representation of the Cummins equation in terms of the parametric model $\hat{\mathbf{K}}(s)$ and the transfer function matrix $\tilde{\mathbf{G}}(s)$:

Table 1
Properties of retardation functions and implications on parametric approximations.

Property	Implication on parametric models
(1) $\lim_{\omega\to 0}\mathbf{K}(j\omega)=\mathbf{0}$	There are zeros at $s=0$
(2) $\lim_{\omega\to\infty}\mathbf{K}(j\omega)=\mathbf{0}$	Strictly proper
(3) $\lim_{t\to 0^+}\mathbf{K}(t)\neq\mathbf{0}$	Relative degree 1
(4) $\lim_{t\to\infty}\mathbf{K}(t)=\mathbf{0}$	Input–output stable
(5) The mapping $\dot{\boldsymbol{\xi}}\mapsto\boldsymbol{\mu}$ is passive	$\mathbf{K}(j\omega)$ is positive real

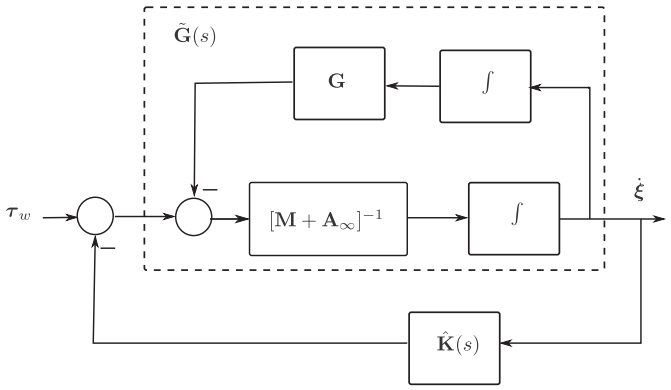

Fig. 1. Block diagram of the Cummins equation in terms of parametric transfer functions.

$$\tilde{\mathbf{G}}(s) = (s^2\mathbf{I} + [\mathbf{M}+\mathbf{A}_\infty]^{-1}\mathbf{G})^{-1}[\mathbf{M}+\mathbf{A}_\infty]^{-1}s. \tag{15}$$

The transfer function matrix $\tilde{\mathbf{G}}(s)$ is passive (Kristiansen et al., 2005). Therefore, the interconnection shown in Fig. 1 will also be passive provided the model $\hat{\mathbf{K}}(s)$ is passive. Here lies the importance of passivity of the identified parametric model. The non-passivity of $\hat{\mathbf{K}}(s)$ does not necessarily imply that the interconnection shown in Fig. 1 will be unstable. However, since the passivity property follows from the hydrodynamics it is desirable to retain this property in the approximating model.

5. Assessing the quality of the model

Once approximating parametric models for the convolution terms are obtained, we need assess how good the impulse and the frequency response are fitted. However, it is also important to check how the added mass and the damping are fitted from the real and imaginary part of the parametric convolution representation (12). That is,

$$\hat{\mathbf{A}}(\omega) = \mathrm{Im}\{\omega^{-1}\hat{\mathbf{K}}(j\omega)\} + \mathbf{A}_\infty, \tag{16}$$

$$\hat{\mathbf{B}}(\omega) = \mathrm{Re}\{\hat{\mathbf{K}}(j\omega)\}, \tag{17}$$

where $\mathrm{Re}\{\cdot\}$ and $\mathrm{Im}\{\cdot\}$ denote the real and imaginary part. In addition to this, one could also check how good the parametric models are with respect to the force-to-displacement frequency response, namely,

$$\mathbf{H}_{f2d}(j\omega) = [-\omega^2[\mathbf{M}+\mathbf{A}(\omega)] + j\omega\mathbf{B}(\omega) + \mathbf{G}]^{-1}. \tag{18}$$

Using the parametric models of the convolution terms (12), we can obtain the transfer function matrix

$$\hat{\mathbf{K}}(s) = \begin{bmatrix} \dfrac{P_{11}(s)}{Q_{11}(s)} & \cdots & \dfrac{P_{16}(s)}{Q_{16}(s)} \\ \vdots & \ddots & \vdots \\ \dfrac{P_{61}(s)}{Q_{61}(s)} & \cdots & \dfrac{P_{66}(s)}{Q_{66}(s)} \end{bmatrix}. \tag{19}$$

It also follows from the Laplace transform of (4) that the force-to-displacement and force-to-velocities transfer functions are

$$\hat{\mathbf{H}}_{f2d}(s) = s^{-1}[\mathbf{I} + \tilde{\mathbf{G}}(s)\hat{\mathbf{K}}(s)]^{-1}\hat{\mathbf{K}}(s), \tag{20}$$

$$\hat{\mathbf{H}}_{f2v}(s) = [\mathbf{I} + \tilde{\mathbf{G}}(s)\hat{\mathbf{K}}(s)]^{-1}\hat{\mathbf{K}}(s). \tag{21}$$

6. Frequency-domain identification of fluid-memory models

Since the hydrodynamic codes provide hydrodynamic data as a function of the frequency, it natural to consider the identification problem *ab initio* in the frequency domain. Furthermore, the frequency-domain methods allow one to incorporate constraints on the model structure and parameters discussed in Section 4. These constraints are not easy to impose in time-domain identification methods (Perez and Fossen, 2008b).

6.1. Complex curve fitting

Consider the non-parametric data $K_{ik}(j\omega_l)$ obtained by evaluating (10) at a finite set of frequencies $l=1,\ldots,N$. By adopting an appropriate order and relative degree for the parametric model (12) (these issues that are addressed in Section 7), the parameter estimation problem can be posed a complex LS curve fitting:

$$\boldsymbol{\theta}^{\star} = \underset{\boldsymbol{\theta}}{\operatorname{argmin}} \sum_l w_l \varepsilon_l^* \varepsilon_l, \tag{22}$$

where the notation * indicates transpose complex conjugate, and

$$\varepsilon_l = K_{ik}(j\omega_l) - \frac{P_{ik}(j\omega_l,\boldsymbol{\theta})}{Q_{ik}(j\omega_l,\boldsymbol{\theta})}, \tag{23}$$

and the vector of parameters $\boldsymbol{\theta}$ is defined as

$$\boldsymbol{\theta} = [p_r, \ldots, p_0, q_{n-1}, \ldots, q_0]^T. \tag{24}$$

The weights w_l can be exploited to select how important is the fit at different frequency ranges. The above parameter estimation problem is a non-linear LS problem in the parameters, which can be solved using a Gauss–Newton algorithm, or it can be linearised as indicated in the next section.

6.2. A linearised iterative solution for complex curve fitting

Levy (1959), proposed a linearisation of (22). That is,

$$\boldsymbol{\theta}'^{\star} = \underset{\boldsymbol{\theta}}{\operatorname{argmin}} \sum_l w'_l (\varepsilon_l'^* \varepsilon'_l), \tag{25}$$

where

$$\varepsilon'_l = Q_{ik}(j\omega_l,\boldsymbol{\theta})\tilde{K}_{ik}(j\omega_l) - P_{ik}(j\omega_l,\boldsymbol{\theta}). \tag{26}$$

This problem is linear in the parameters, and thus easy to solve. Indeed, using a matrix form we can write

$$\boldsymbol{\theta}'^{\star} = \underset{\boldsymbol{\theta}}{\operatorname{argmin}}\, \boldsymbol{\varepsilon}'^* \mathbf{W} \boldsymbol{\varepsilon}', \tag{27}$$

with

$$\boldsymbol{\varepsilon}' = [\varepsilon'_1, \ldots, \varepsilon'_N]^T, \quad \mathbf{W} = \operatorname{diag}(w'_1, w'_2, \ldots, w'_n). \tag{28}$$

Using this notation, we can write

$$\boldsymbol{\varepsilon}' = \boldsymbol{\Gamma} - \boldsymbol{\Phi}\boldsymbol{\theta}, \tag{29}$$

with the obvious definition for the matrices $\boldsymbol{\Phi}$ and $\boldsymbol{\Gamma}$.

The solution to (27)–(29) is then given by

$$\boldsymbol{\theta}'^{\star} = (\boldsymbol{\Phi}^T \mathbf{W} \boldsymbol{\Phi})^{-1} \boldsymbol{\Phi}^T \mathbf{W} \boldsymbol{\Gamma}. \tag{30}$$

The linearised problem (25) derives from the non-linear problem (22) by choosing

$$w_l = w'_l |Q(j\omega_l,\boldsymbol{\theta})|^2. \tag{31}$$

This means that solving (25) can be thought as solving (22) with the weights as given in (31). A problem with this linear formulation is that the identified transfer function does not in general give a good fitting. For example, when the data extend over a large range of frequencies or when $Q(s)$ has poorly damped complex roots close to the imaginary axis, the coefficients w_l in (31) will weight the fitting more heavily at high frequencies and less heavily at low frequencies and those close to the resonant roots. This weighting normally gives a bias in the parameter estimates.

Sanathanan and Koerner (1963) proposed a method to compensate for the bias in the parameter estimates introduced by the linearisation. This method consists in solving (27)–(29) iteratively using as weighting coefficients the inverse of the denominator $Q(j\omega,\boldsymbol{\theta})$ evaluated at the previous estimate. This algorithm can be summarised in the following:

1. set $\mathbf{W}_0 = \mathbf{I}$,
2. solve $\boldsymbol{\theta}_n^{\star} = \operatorname{argmin}_{\boldsymbol{\theta}} \boldsymbol{\varepsilon}'^* \mathbf{W}_n \boldsymbol{\varepsilon}'$,
3. set $\mathbf{W}_{n+1} = \operatorname{diag}\,(|Q_{ik}(j\omega_l,\boldsymbol{\theta}_n)|^{-2})$ go to 2 until convergence.

This choice of weighting coefficients in step 3 results in the following problem at each step n of the iteration:

$$\boldsymbol{\theta}_n^{\star} = \underset{\boldsymbol{\theta}}{\operatorname{argmin}} \sum_l \left| \frac{Q_{ik}(j\omega_l,\boldsymbol{\theta}) K_{ik}(j\omega_l)}{Q_{ik}(j\omega_l,\boldsymbol{\theta}_{n-1}^{\star})} - \frac{P_{ik}(j\omega_l,\boldsymbol{\theta})}{Q_{ik}(j\omega_l,\boldsymbol{\theta}_{n-1}^{\star})} \right|^2. \tag{32}$$

For data with low level of noise convergence is reached after a few iterations (10–20), $\boldsymbol{\theta}_n^{\star} \approx \boldsymbol{\theta}_{n-1}^{\star}$; and thus, the original non-linear LS problem (22) is approximately recovered (Unbehauen and Rao, 1987).

7. Practical issues associated with the identification of fluid-memory approximations

7.1. Preparing the data

Since the retardation functions relate the velocities to the radiation forces, the numerator coefficients in 12 can take large values compared to those of the denominator. This can result in a numerically ill-conditioned problem 32. To avoid numerical problems, it is convenient to scale the data before performing the identification:

$$K'_{ik}(j\omega) = \alpha K_{ik}(j\omega) \tag{33}$$

with

$$\alpha \triangleq \frac{1}{\max|K_{ik}(j\omega)|}. \tag{34}$$

That is, one should fit a rational transfer function to $K'_{ik}(j\omega)$ and then multiply the resulting numerator by α^{-1} to obtain our estimate of $K_{ik}(j\omega)$. The accuracy of the data has obviously a significant bearing on the identification. Thus, whenever the data at a range of frequencies is believed to be inaccurate, it should not be used for identification. It is also important to eliminate wild points, which may arise from irregular frequencies related to the solution of the boundary-value problem solved by the hydrodynamic code (Faltinsen, 1990). These irregularities in the data can be inspected visually from the plots of added mass $A_{ik}(j\omega)$ and potential damping $B_{ik}(j\omega)$ of each entry.

7.2. Adding prior knowledge

Based on the information provided in Table 1, it follows that the rational transfer functions 12 have

- a zero at $s=0$,
- relative degree 1, i.e., $r=n-1$ where $n=\deg(Q)$, and $r=\deg(P)$.

The constraint that the functions have a zero at $s=0$, can be addressed by "integrating" the data in the frequency domain.

Indeed, we can factorise

$$P_{ik}(s) = sP'_{ik}(s), \tag{35}$$

where $P'_{ik}(s)$ does not have roots on the imaginary axis of the complex plane and has degree $\deg(P'_{ik}) = n-2$. Then, we can express (12) as follows:

$$\hat{K}_{ik}(j\omega) = \frac{(j\omega)P'_{ik}(j\omega,\boldsymbol{\theta}_{ik})}{Q_{ik}(j\omega,\boldsymbol{\theta}_{ik})}. \tag{36}$$

We can further divide (36) by $j\omega$, which is the equivalent of integrating the data in the time domain,

$$\frac{\hat{K}_{ik}(j\omega)}{(j\omega)} = \frac{P'_{ik}(j\omega,\boldsymbol{\theta}_{ik})}{Q_{ik}(j\omega,\boldsymbol{\theta}_{ik})}, \tag{37}$$

and then fit

$$\boldsymbol{\theta}^{\star}_{ik} = \underset{\boldsymbol{\theta}}{\operatorname{argmin}} \sum_l \left| \frac{K_{ik}(j\omega_l)}{(j\omega_l)} - \frac{P'_{ik}(j\omega_l,\boldsymbol{\theta})}{Q_{ik}(j\omega_l,\boldsymbol{\theta})} \right|^2. \tag{38}$$

Since the LS method discussed in Sections 6.1 and 6.2 was introduced for a general case, this simply implies that we need to chose only the order n to apply the method with $r=n-2$. Then after $P'_{ik}(s)$ is identified, the factor s can be incorporated to the numerator polynomial to form $P_{ik}(s)$ according to (35).

7.3. Order selection

The order of the transfer functions depends on the hydrodynamic characteristics of the vessel or marine structure, i.e., it depends on the hull shape. Based on the properties of the convolution terms given in Table 1, it follows that the minimum order transfer function that satisfies all the properties is a second order one:

$$\hat{K}^{\min}_{ik}(s) = \frac{p_0 s}{s^2 + q_1 s + q_0}. \tag{39}$$

Therefore, one can start with this minimum order transfer function ($n=2$), and increase the order while monitoring that the LS cost decreases—or simply by visual inspection of the fitted frequency response and the added mass and damping computed from the approximation as indicated in (16) and (17). If the order of the proposed model is too large, there will be over-fitting; and therefore, near zero-pole cancellations. In the toolbox developed by Perez and Fossen (2009), the estimation starts with the second order model (39), and then the coefficient of determination R^2 is used to evaluate the quality of the fitting of the added mass and also damping. The order of the approximation is increased iterative until both coefficients of determination are above 0.99. Then, the user has the option to adjust the order further. This method has been evaluated using data of several marine structures, and it has not produced over-fitting.

7.4. Stability

The resulting model from the LS minimization may not necessarily be stable because stability is not enforced as a constraint in the optimisation. This can be addressed after the identification. Should the obtained model be unstable, one could obtain a stable one by reflecting the unstable poles about the imaginary axis and re-computing the denominator polynomial. That is,

(i) compute the roots of $\lambda_1, \ldots, \lambda_n$ of $Q_{ik}(s,\hat{\boldsymbol{\theta}}_{ik})$,
(ii) if Re $\{\lambda_i\} > 0$, then set Re $\{\lambda_i\} = -$ Re $\{\lambda_i\}$,
(iii) reconstruct the polynomial: $Q_{ik}(s) = (s-\lambda_1)(s-\lambda_1), \cdots, (s-\lambda_n)$.

When the validity of the model is assessed, this should be done with a stable model.

7.5. Passivity

A disadvantage of the method of LS curve fitting is that it does not enforce passivity. If passivity is required (i.e., $B_{ik}(\omega) > 0$), a simple way to ensure it is to try different order approximations and choose the one that is passive. The approximation is passive if

$$\operatorname{Re}\left\{ \frac{P_{ik}(j\omega_l,\boldsymbol{\theta})}{Q_{ik}(j\omega_l,\boldsymbol{\theta})} \right\} > 0. \tag{40}$$

When this is checked, one should evaluate the transfer function at low and high frequencies—below and above the frequencies used for the parameter estimation.

Normally, low-order approximation models of the convolution terms given by this method are passive—the term "low" depends on the data of the particular vessel under consideration. Therefore, one can reduce the order and trade-off fitting accuracy for passivity. A different approach would be optimise the numerator of the obtained non-passive model to obtain a passive approximation—this goes beyond the scope of this paper, but the reader is referred to Damaren (2000) and references therein.

7.6. Summary of a practical algorithm for the identification fluid-memory models

To summarise the identification process based on LS-fitting of the frequency response of the retardation functions, taking into consideration all the issues discussed in the previous section, we present the following algorithm:

1. Set the appropriate range of frequencies where the hydrodynamic data are considered accurate, eliminate wild points, and compute the frequency response for a set of frequencies ω_l:
$$K_{ik}(j\omega_l) = B_{ik}(\omega_l) - j\omega(A_{ik}(\omega_l) - A_{\infty,ik}). \tag{41}$$
2. Scale the data:
$$K_{ik}{}'(j\omega_l) = \alpha K_{ik}(j\omega_l), \quad \alpha \triangleq \frac{1}{\max|K_{ik}(j\omega_l)|}. \tag{42}$$
3. Select the order of the approximation $n = \deg(Q_{ik}(j\omega,\boldsymbol{\theta}_{ik}))$. The minimum order approximation $n=2$ can be the starting point.
4. Estimate the parameters
$$\boldsymbol{\theta}^{\star}_{ik} = \underset{\boldsymbol{\theta}}{\operatorname{argmin}} \sum_l \left| \frac{K'_{ik}(j\omega_l)}{(j\omega_l)} - \frac{P'_{ik}(j\omega_l,\boldsymbol{\theta})}{Q_{ik}(j\omega_l,\boldsymbol{\theta})} \right|^2, \tag{43}$$
with $\deg(P'_{ik}(j\omega,\boldsymbol{\theta}_{ik})) = n-2$. Use the iterative linear LS solution described in Section 6.2.
5. Check stability by computing the roots of $Q_{ik}(j\omega,\boldsymbol{\theta}^{\star}_{ik})$ and change the real part of those roots with positive real part—see Section 7.
6. Construct the desired transfer function by scaling and incorporate the s factor in the numerator:
$$\hat{K}_{ik}(s) = \frac{1}{\alpha} \frac{sP'_{ik}(s,\boldsymbol{\theta}^{\star}_{ik})}{Q_{ik}(s,\boldsymbol{\theta}^{\star}_{ik})}. \tag{44}$$
7. Estimate the added mass and damping based on the identified parametric approximation via
$$\hat{A}_{ik}(\omega) = \operatorname{Im}\{\omega^{-1}\hat{K}_{ik}(j\omega)\} + A_{\infty,ik} \tag{45}$$
$$\hat{B}_{ik}(\omega) = \operatorname{Re}\{\hat{K}_{ik}(j\omega)\}, \tag{46}$$
and compare with the $A_{ik}(\omega)$ and $B_{ik}(\omega)$ given by the hydrodynamic code. If the fitting is not satisfactory increase the order of the approximation and go back to step (iii).
8. Check for passivity if required $\hat{B}_{ik}(j\omega) > 0$.

8. Joint identification of infinite-frequency added mass and fluid-memory models

Most commercial hydrodynamic codes based on strip theory do not normally provide the value of the infinite-frequency added mass coefficient $\mathbf{A}_\infty = \lim_{\omega\to\infty}\mathbf{A}(\omega)$. In these cases, we cannot form $\mathbf{K}(j\omega)$ as indicated in (10). Perez and Fossen (2008a) proposed a method exploits the knowledge and methods used in the identification of $\hat{K}_{ik}(s)$ discussed in the previous section; and therefore, it provides a natural extension of those results putting the two identification problems into the same framework.

The frequency-domain representation of the radiation forces given in (5) can be alternatively expressed as

$$\tau_{rad,ik}(j\omega) = \left[\frac{B_{ik}(\omega)}{j\omega} + A_{ik}(\omega)\right]\ddot{\xi}(s), \tag{47}$$

where the expression in brackets gives the complex coefficient

$$\tilde{A}(j\omega) \triangleq \frac{B_{ik}(\omega)}{j\omega} + A_{ik}(\omega). \tag{48}$$

From the Laplace transform of (3), and a rational approximation for the convolution term, it also follows that

$$\hat{\tau}_{rad,ik}(s) = \left[A_{\infty,ik}s + \frac{P_{ik}(s)}{Q_{ik}(s)}\right]\dot{\xi}(s), \tag{49}$$

$$= \left[A_{\infty,ik} + \frac{P'_{ik}(s)}{Q_{ik}(s)}\right]\ddot{\xi}(s), \tag{50}$$

with $P_{ik}(s) = sP'_{ik}(s)$. This representation can be traced back to the work of Söding (1982), and it has been used by Xia et al. (1998) and Sutulo and Guedes-Soares (2005), but with a different approach to that presented in this paper.

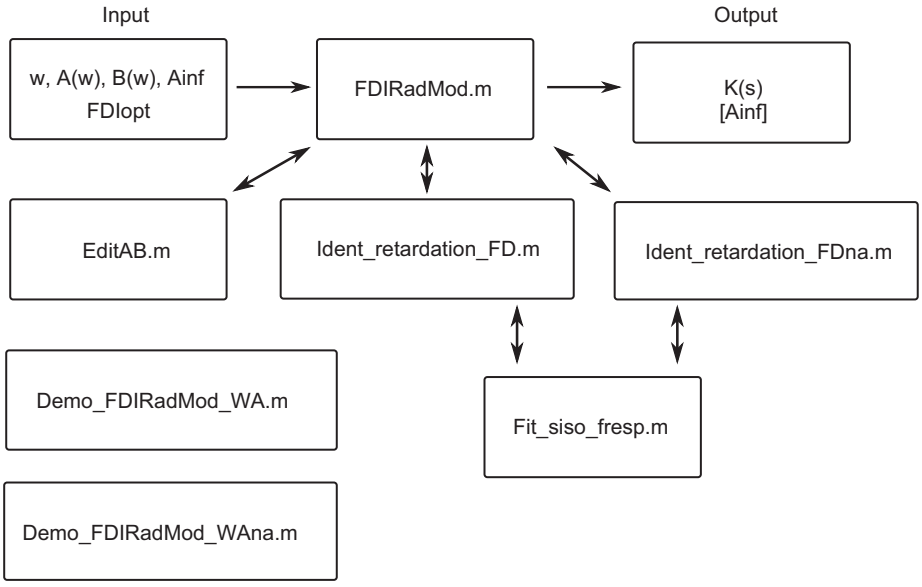

Fig. 2. Organisation of the MSS-FDI toolbox for frequency-domain identification of radiation models of marine structures (www.marinecontrol.org).

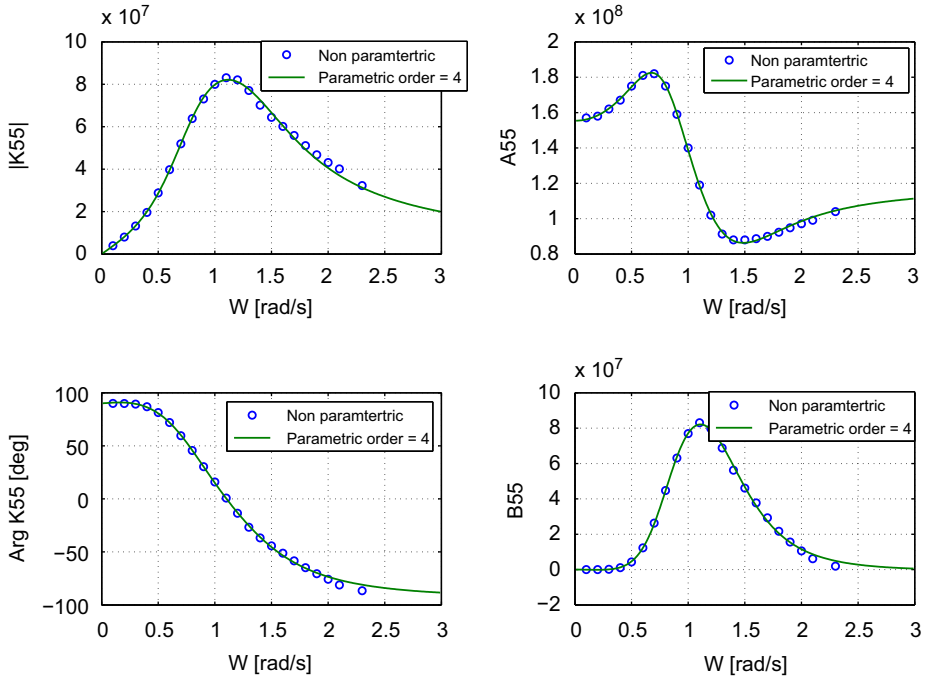

Fig. 3. Results of a 4th-order parametric approximation of the convolution term in pitch.

The transfer function in brackets in (50) can be further expressed as

$$\hat{\tilde{A}}_{ik}(s)=\frac{R_{ik}(s)}{S_{ik}(s)}=\frac{A_{\infty,ik}Q_{ik}(s)+P_{ik}(s)}{Q_{ik}(s)}, \tag{51}$$

from which it follows that $\deg(R_{ik})=\deg(S_{ik})=n$. Therefore, we can follow the same approach as in Section 6 and use LS optimisation to estimate the parameters of the polynomial R_{ik} and S_{ik} given the frequency-response data (48):

$$\boldsymbol{\theta}^\star=\underset{\boldsymbol{\theta}}{\operatorname{argmin}}\sum_l w_l(\varepsilon_l^*\varepsilon_l), \tag{52}$$

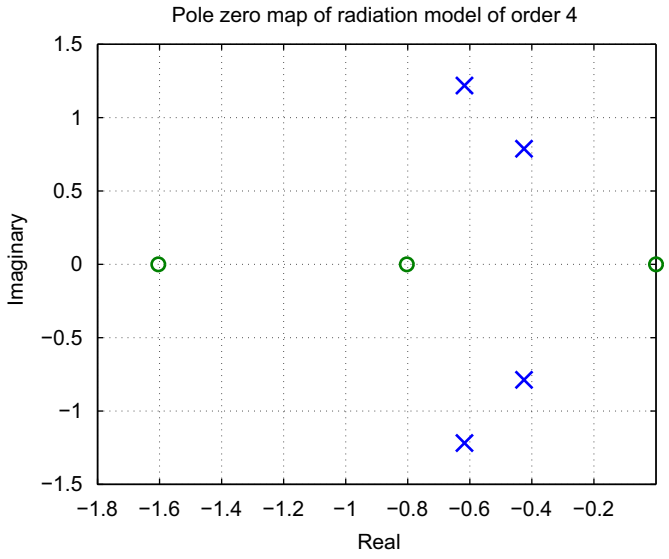

Fig. 4. Pole-zero map of the 4th-order parametric approximation of the convolution term in pitch.

with

$$\varepsilon_l=\tilde{A}_{ik}(j\omega_l)-\frac{R_{ik}(j\omega_l,\boldsymbol{\theta})}{S_{ik}(j\omega_l,\boldsymbol{\theta})}, \tag{53}$$

with the constraint that $n=\deg S_{ik}(s)=\deg R_{ik}(s)$. We also know from Section 7 that the minimum order approximation is of $n=2$. Therefore, we can start with this order and increment to improve the fit if necessary.

It should be noted as well that if we normalised the polynomial $S_{ik}(s)$ to be monic as $Q_{ik}(s)$ is in (12), then

$$\hat{A}_{\infty,ik}=\lim_{\omega\to\infty}\frac{R_{ik}(s,\boldsymbol{\theta}^\star)}{S_{ik}(s,\boldsymbol{\theta}^\star)}, \tag{54}$$

that is, the infinite-frequency added mass $\hat{A}_{\infty,ik}$ is the coefficient of the highest order term of $R_{ik}(s,\boldsymbol{\theta}^\star)$.

Therefore, after obtaining $R_{ik}(s,\boldsymbol{\theta}^\star)$ and $S_{ik}(s,\boldsymbol{\theta}^\star)$, we can recover the polynomials for the fluid-memory model together with the infinite added mass coefficients:

$$Q_{ik}(s,\boldsymbol{\theta}^\star)=S_{ik}(s,\boldsymbol{\theta}^\star),$$

$$P_{ik}(s,\boldsymbol{\theta}^\star)=R_{ik}(s,\boldsymbol{\theta}^\star)-\hat{A}_{\infty,ik}S_{ik}(s,\boldsymbol{\theta}^\star). \tag{55}$$

Perez and Fossen (2008a) show examples where the above method provides estimates of the infinite-frequency added mass coefficients that are well within 10% of the coefficients computed by 3D-code WAMIT.

9. MSS-FDI toolbox

Perez and Fossen (2009) developed a MATLAB toolbox for frequency-domain identification (FDI) of radiation force models of marine structures. This toolbox, which is freely available at www.marinecontrol.org, implements the estimation algorithms described in the previous sections, and it incorporates extra tools to prepare the data for estimation. Fig. 2 shows a diagram of the different software components of the toolbox and their

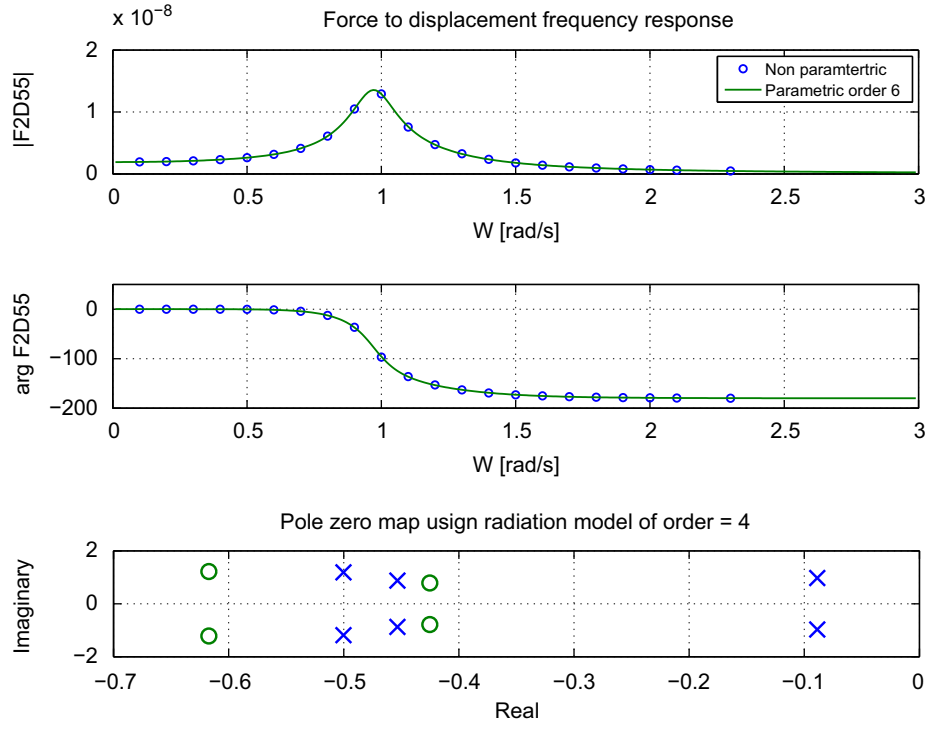

Fig. 5. Force-to-displacement frequency response function and pole-zero map corresponding to a 4th-order parametric approximation of the convolution term.

dependability. The main function of the toolbox is `FDIRadMod.m`, which processes the input data and returns the estimate of the fluid-memory transfer function approximation with auto-order selection and also estimates the infinite-frequency added mass if required. This function calls other functions to prepare the data for identification, which allow selecting the desired range of frequencies used in the estimation, and also allow elimination of data points. The toolbox also includes two demos which show how to use the main functions. The first demo considers the estimation with infinite-frequency added mass available (WA), and the second demo considers the estimation without using infinite-frequency added mass value (NA). In the following section, we use the toolbox with a particular example.

10. On accuracy of radiation force models and low-order approximations

In this section, we consider hydrodynamic data of an ellipsoidal hull in the degree of freedom of pitch, which due to symmetry can

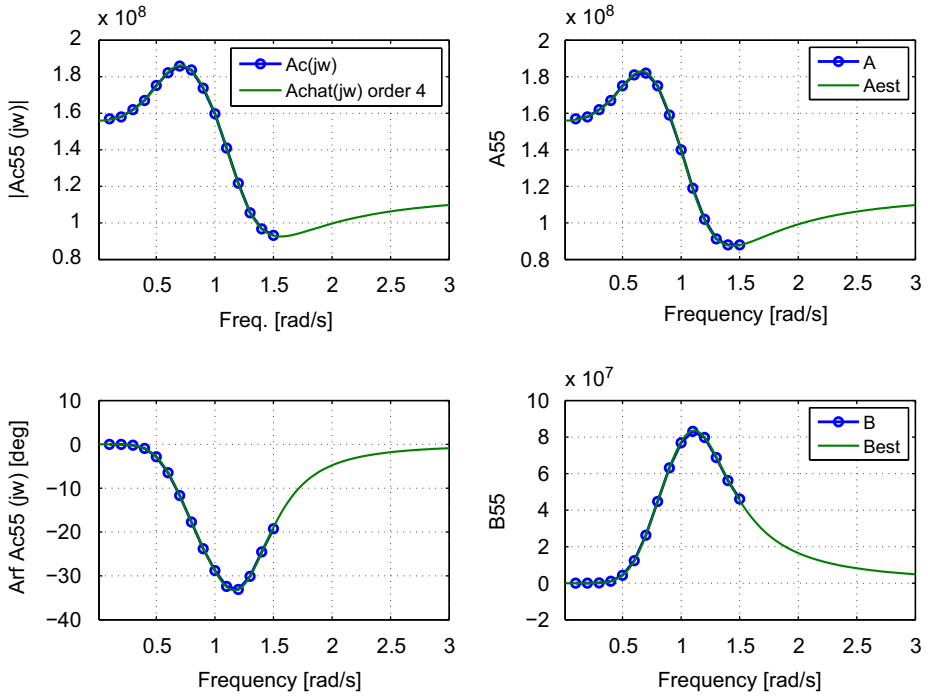

Fig. 6. Results of a 4th-order parametric approximation for joint convolution and infinite-frequency added mass estimation.

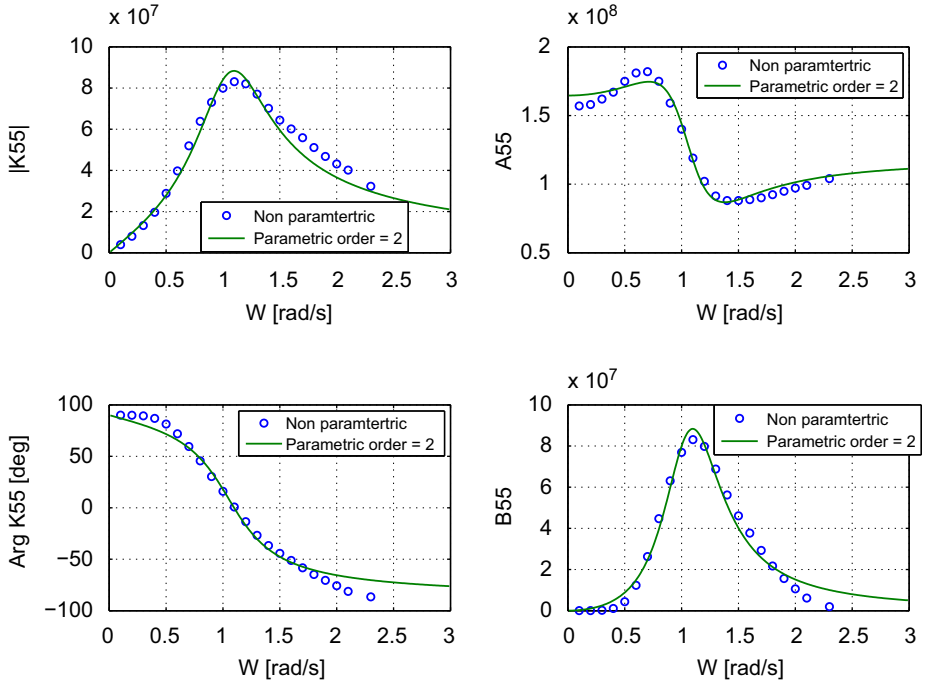

Fig. 7. Results of a 2nd-order parametric approximation of the convolution term in pitch.

be de-coupled from other degrees of freedom. We use this example to illustrate the results obtained using the MSS-FDI toolbox. In addition, we use the example to show that if a force-to-motion model is sought, which is often the case except for analysis wave-energy converters, then it may not be necessary to have an accurate model of the fluid-memory term.

Fig. 3 shows the estimation results using a parametric model approximation of order $n=4$. This is the result of the auto-order selection implemented in the toolbox, which is based on the coefficient of determination of the added mass and damping fit.

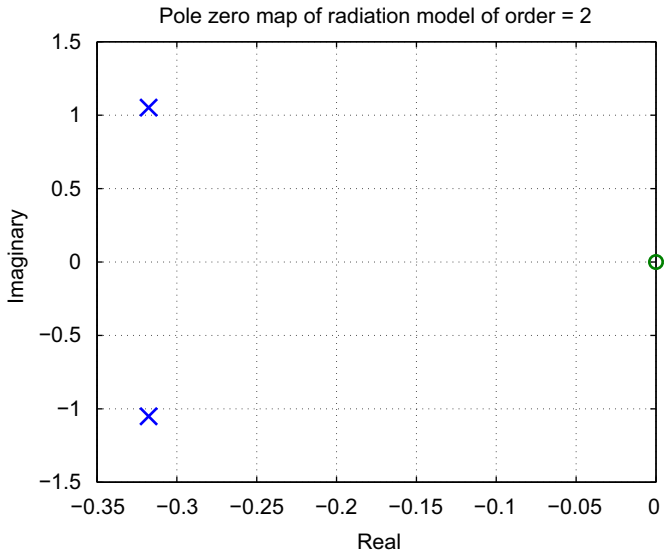

Fig. 8. Pole-zero map of the 2nd-order parametric approximation of the convolution term in pitch.

The left-hand plots show the fitting of the convolution frequency response, and the right-hand plots show the reconstructed added mass and damping. Fig. 4 shows the poles and the zeros of the parametric model approximation. Fig. 5 shows the fit of the force-to-motion (pitch moment to pitch angle) frequency response given by (20), and the bottom plot shows the resulting pole-zero map. Fig. 6 shows the fitting results obtained without using information related to the infinite-frequency added mass coefficient. In this case, the estimation of infinite-frequency added mass was within 1% of that provided by the hydrodynamic code.

Figs. 7–9 show the fitting results of a convolution approximation of order $n=2$, which is the lowest order approximation that we can consider. From Figs. 3 and 7, we can see that neither the convolution frequency response nor the reconstruction of the added mass and damping corresponding to the 2nd-order convolution approximation are as accurate as the results of the 4th-order convolution approximation. Despite this, Figs. 5 and 9 show a force-to-motion models with similar accuracy. This is the result of the motion of the poles and the zeros due to the feedback interconnection of the models $\tilde{G}(s)$ and $\hat{K}(s)$—see Fig. 1. This gives rise to a separation of the poles of the force-to-motion model, which results in a pair complex-conjugate poles that dominate the response. Indeed, from the pole–zero maps in Figs. 5 and 9, we can see that there is a dominant pair of complex-conjugate poles which remain relatively invariant with respect to the different approximations of the convolution terms. Therefore, it is expected that both force-to-motion frequency responses be similar.

The above results indicate that if a force-to-motion model is sought, then it is usually unnecessary to have an accurate convolution approximation models since the high-order dynamics that go into these approximations are dominated by a low-order dynamic model in the force-to-motion response. This effect has been observed by the authors in several examples of offshore structures. This has motivated the proposal of using direct force-to-motion identification in order to reduce the order of the models (Perez and Lande, 2006).

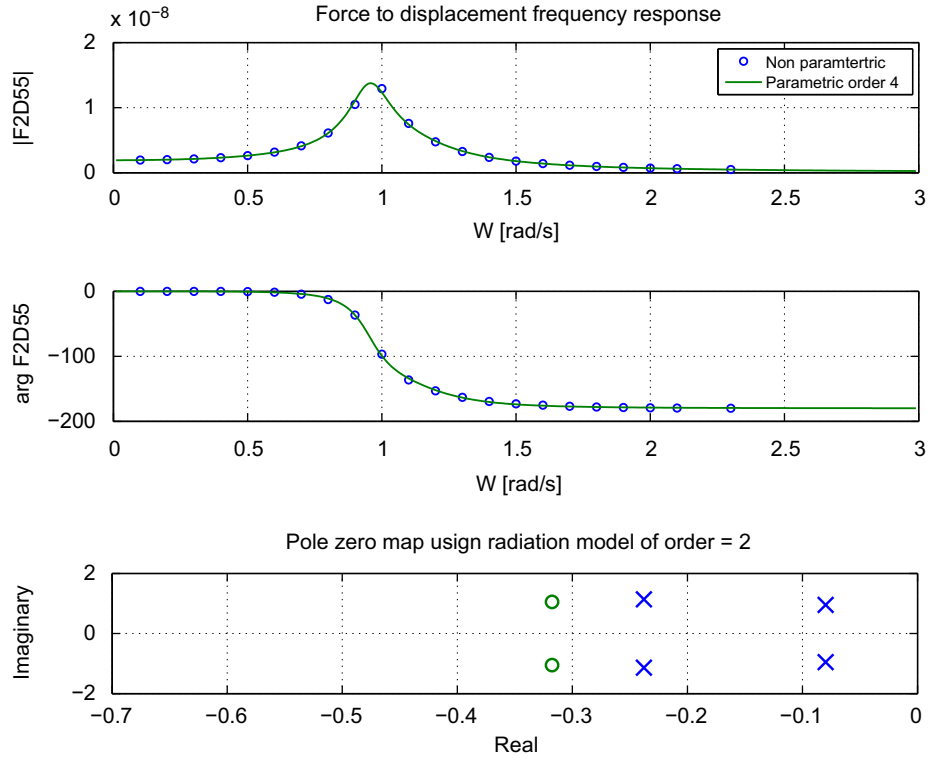

Fig. 9. Force-to-displacement frequency response function and pole-zero map corresponding to a 2nd-order parametric approximation of the convolution term.

11. Conclusions

Recent work has highlighted that frequency-domain methods for identification of approximating linear parametric models of dynamic response of marine structures are simple to implement and allow incorporating model structure constraints. This paper summarises these estimation algorithms, which due to the use of constraints lead to approximating models that satisfy the physical properties associated with the phenomenon involved. We use an illustration example and obtain different approximating models using a freely available MATLAB toolbox that implements the estimation algorithms described in the paper. In this example, we use both a low- and a high-order approximations for the convolution term, and highlight that both lead to force-to-motion models with similar accuracy. This study indicates that if one is interested in a force-to-motion model, which is often the ultimate modelling objective, there may be no need to have a very accurate model of convolution terms since the high-order dynamics are usually dominated by a low-order dynamic model.

References

Beck, R., Reed, A., 2001. Modern computational methods for ships in a seaway. SNAME Transactions 109, 1–51.

Cummins, W., 1962. The impulse response function and ship motion. Technical Report 1661, David Taylor Model Basin–DTNSRDC.

Damaren, C., 2000. Time-domain floating body dynamics by rational approximations of the radiation impedance and diffraction mapping. Ocean Engineering 27, 687–705.

Faltinsen, O., 1990. Sea Loads on Ships and Offshore Structures. Cambridge University Press.

Hjulstad, A., Kristansen, E., Egeland, O., 2004. State-space representation of frequency-dependant hydrodynamic coefficients. In: Proceedings of IFAC Conference on Control Applications in Marine Systems.

Holappa, K., Falzarano, J., 1999. Application of extended state space to nonlinear ship rolling. Ocean Engineering 26, 227–240.

Jefferys, E., Broome, D., Patel, M., 1984. A transfer function method of modelling systems with frequency dependent coefficients. Journal of Guidance Control and Dynamics 7 (4), 490–494.

Jefferys, E., Goheen, K., 1992. Time domain models from frequency domain descriptions: application to marine structures. International Journal of Offshore and Polar Engineering 2, 191–197.

Jordan, M., Beltran-Aguedo, R., 2004. Optimal identification of potential-radiation hydrodynamics of moored floating structures. Ocean Engineering 31, 1859–1914.

Kailath, T., 1980. Linear Systems. Prentice-Hall.

Khalil, H., 2000. Nonlinear Systems. Prentice-Hall.

Kristansen, E., Egeland, O., 2003. Frequency dependent added mass in models for controller design for wave motion ship damping. In: Sixth IFAC Conference on Manoeuvring and Control of Marine Craft MCMC'03, Girona, Spain.

Kristiansen, E., Hjuslstad, A., Egeland, O., 2005. State-space representation of radiation forces in time-domain vessel models. Ocean Engineering 32, 2195–2216.

Levy, E., 1959. Complex curve fitting. IRE Transactions on Automatic Control AC 4, 37–43.

McCabe, A., Bradshaw, A., Widden, M., 2005. A time-domain model of a floating body using transforms. In: Proceedings of Sixth European Wave and Tidal energy Conference, University of Strathclyde, Glasgow, U.K., August.

Newman, J., 1977. Marine Hydrodynamics. MIT Press.

Ogilvie, T., 1964. Recent progress towards the understanding and prediction of ship motions. In: Sixth Symposium on Naval Hydrodynamics.

Perez, T., Fossen, T., 2008a. Joint identification of infinite-frequency added mass and fluid-memory models of marine structures. Modeling Identification and Control 29 (3), 93–102. doi:10.4173/mic.2008.1.1.

Perez, T., Fossen, T.I, 2008b. Time-domain vs. frequency-domain identification of parametric radiation force models for marine structures at zero speed. Modeling Identification and Control 29 (1), 1–19. doi:10.4173/mic.2008.3.2.

Perez, T., Fossen, T.I., 2009. A matlab toolbox for parametric identification of radiation-force models of ships and offshore structures. Modeling Identification and Control 30 (1), 1–15. doi:10.4173/mic.2009.1.1.

Perez, T., Lande, Ø., 2006. A frequency-domain approach to modelling and identification of the force to motion vessel response. In: Proceedings of Seventh IFAC Conference on Manoeuvring and Control of Marine Craft, Lisbon, Portugal.

Salvesen, N., Tuck, E., Faltinsen, O., 1970. Ship motions and sea loads. Transactions of the Society of Naval Architects and Marine Engineers—SNAME 10, 345–356.

Sanathanan, C., Koerner, J., 1963. Transfer function synthesis as a ratio of two complex polynomials. IEEE Transactions of Automatic Control 8 (1), 56–58. doi:10.1109/TAC.1963.1105517.

Söding, H., 1982. Leckstabilität im seegang. Technical Report, Report 429 of the Institue für Schiffbau, Hamburg.

Sutulo, S., Guedes-Soares, C., 2005. An implementation of the method of auxiliary state variables for solving seakeeping problems. International Shipbuilding Progress 52 (4), 357–384.

Taghipour, R., Perez, T., Moan, T., 2007. Time domain hydroelastic analysis of a flexible marine structure using state-space models. In: 26th International Conference on Offshore Mechanics and Arctic Engineering—OMAE 07, San Diego, CA, USA.

Taghipour, R., Perez, T., Moan, T., 2008. Hybrid frequency–time domain models for dynamic response analysis of marine structures. Ocean Engineering 35 (7), 685–705. doi:10.1016/j.oceaneng.2007.11.002.

Unbehauen, H., Rao, G.P., 1987. Identification of Continuous Systems. Systems and Control Series. vol. 10, North-Holland.

Xia, J., Wang, Z., Jensen, J., 1998. Nonlinear wave-loads and ship responses by a time-domain strip theory. Marine Structures 11, 101–123.

Yu, Z., Falnes, J., 1995. Spate-space modelling of a vertical cylinder in heave. Applied Ocean Research 17, 265–275.

Yu, Z., Falnes, J., 1998. State-space modelling of dynamic systems in ocean engineering. Journal of hydrodynamics, 1–17.